University of Nebraska - Lincoln
DigitalCommons@University of Nebraska - Lincoln

Faculty Publications from the Department of Electrical and Computer Engineering

Electrical & Computer Engineering, Department of

7-16-2014

Thickness determination of few-layer hexagonal boron nitride films by scanning electron microscopy and Auger electron spectroscopy

P. Sutter
Brookhaven National Laboratory, psutter@unl.edu

E. Sutter
Brookhaven National Laboratory, esutter@unl.edu

Follow this and additional works at: http://digitalcommons.unl.edu/electricalengineeringfacpub

Part of the Computer Engineering Commons, and the Electrical and Computer Engineering Commons

Sutter, P. and Sutter, E., "Thickness determination of few-layer hexagonal boron nitride films by scanning electron microscopy and Auger electron spectroscopy" (2014). *Faculty Publications from the Department of Electrical and Computer Engineering*. 449.
http://digitalcommons.unl.edu/electricalengineeringfacpub/449

This Article is brought to you for free and open access by the Electrical & Computer Engineering, Department of at DigitalCommons@University of Nebraska - Lincoln. It has been accepted for inclusion in Faculty Publications from the Department of Electrical and Computer Engineering by an authorized administrator of DigitalCommons@University of Nebraska - Lincoln.

Thickness determination of few-layer hexagonal boron nitride films by scanning electron microscopy and Auger electron spectroscopy

P. Sutter, and E. Sutter

Citation: APL Materials **2**, 092502 (2014); doi: 10.1063/1.4889815
View online: https://doi.org/10.1063/1.4889815
View Table of Contents: http://aip.scitation.org/toc/apm/2/9
Published by the American Institute of Physics

Articles you may be interested in

Optical thickness determination of hexagonal boron nitride flakes
Applied Physics Letters **102**, 161906 (2013); 10.1063/1.4803041

Fast pick up technique for high quality heterostructures of bilayer graphene and hexagonal boron nitride
Applied Physics Letters **105**, 013101 (2014); 10.1063/1.4886096

Electron tunneling through atomically flat and ultrathin hexagonal boron nitride
Applied Physics Letters **99**, 243114 (2011); 10.1063/1.3662043

Making graphene visible
Applied Physics Letters **91**, 063124 (2007); 10.1063/1.2768624

The two-dimensional phase of boron nitride: Few-atomic-layer sheets and suspended membranes
Applied Physics Letters **92**, 133107 (2008); 10.1063/1.2903702

Two-dimensional van der Waals materials
Physics Today **69**, 38 (2016); 10.1063/PT.3.3297

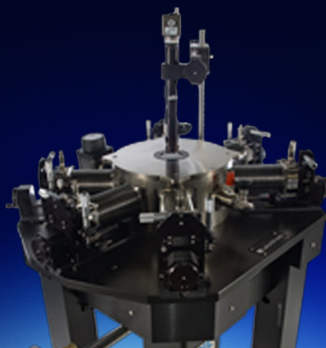

APL MATERIALS **2**, 092502 (2014)

Thickness determination of few-layer hexagonal boron nitride films by scanning electron microscopy and Auger electron spectroscopy

P. Sutter[a] and E. Sutter
Center for Functional Nanomaterials, Brookhaven National Laboratory, Upton, New York 11973, USA

(Received 21 May 2014; accepted 30 June 2014; published online 16 July 2014)

We assess scanning electron microscopy (SEM) and Auger electron spectroscopy (AES) for thickness measurements on few-layer hexagonal boron nitride (h-BN), the layered dielectric of choice for integration with graphene and other two-dimensional materials. Observations on h-BN islands with large, atomically flat terraces show that the secondary electron intensity in SEM reflects monolayer height changes in films up to least 10 atomic layers thickness. From a quantitative analysis of AES data, the energy-dependent electron escape depth in h-BN films is deduced. The results show that AES is suitable for absolute thickness measurements of few-layer h-BN of 1 to 6 layers. © *2014 Author(s). All article content, except where otherwise noted, is licensed under a Creative Commons Attribution 3.0 Unported License.* [http://dx.doi.org/10.1063/1.4889815]

Two-dimensional materials,[1] such as graphene, hexagonal boron nitride (h-BN), and a family of transition metal dichalcogenides (MX_2) have attracted significant interest for their electronic, optical, chemical, and mechanical properties. Positioned between 2D materials and the bulk crystals from which they are derived, layered materials with several atomic layers are increasingly recognized for their unique properties, which are typically different from those of the monolayers[2] and the bulk and often vary substantially with thickness.[3,4] Hexagonal boron nitride (h-BN), a layered insulator with a bandgap of nearly 6 eV,[5] whose surface is both topographically flat and contains a low density of scattering centers for charge carriers,[6] is expected to play a key role in a range of emerging applications. For example, graphene supported on few-layer h-BN has shown record carrier mobilities,[7] and h-BN is the substrate of choice for exploring new physical phenomena associated with low-dimensional charge carriers in graphene[8] and other 2D materials.[9] Heterostructures comprising few-layer h-BN sandwiched between graphene layers are being explored for novel tunneling devices.[10]

To harness the desired dielectric properties, h-BN films with a uniform thickness of several atomic layers are often required. A precise thickness measurement is therefore among the most important elements of h-BN metrology, irrespective of the approach used to fabricate the few-layer films. For h-BN exfoliated from bulk crystals, optical reflectivity provides quantitative thickness information,[11,12] but it requires a special substrate—typically SiO_2/Si with a well-defined oxide thickness—to enhance the optical contrast. Recently, different approaches have been developed for the scalable synthesis of monolayer[13–16] or few-layer[17,18] h-BN on metal substrates. In this context, methods are needed for determining the thickness of h-BN layers while still supported on the metal substrate, or alternatively after transfer to a different support, which may not necessarily be SiO_2/Si.

Here, we establish the basis for using scanning electron microscopy (SEM) and Auger electron spectroscopy (AES) to measure the thickness of few-layer h-BN. SEM is available in many research laboratories and enables facile mapping of surfaces. AES is a well-established surface science

[a]Author to whom correspondence should be addressed. Electronic mail: psutter@bnl.gov

 © Author(s) 2014

method for elemental and chemical analysis that can be used for both spatially averaging and local measurements. If a focused electron beam is used to excite Auger electrons, AES measurements can be performed within nanometer areas. In the context of thickness measurements, the inelastic mean free path (IMFP) of Auger electrons, which determines the electron escape depth and hence governs the film thicknesses that can be measured reliably, is a key parameter in the quantitative analysis of AES data. While the so-called "universal curve" provides approximate values of the energy-dependent IMFP ($\lambda(E)$), measured values for particular materials and crystal structures are required for metrology applications.

To explore the potential of SEM and AES for h-BN thickness characterization, we have synthesized few-layer h-BN samples on Ru(0001)/Al_2O_3(0001) thin films using a recently demonstrated growth method based on reactive magnetron sputtering of boron in N_2/Ar, which has allowed us to achieve the controlled growth of high-quality few-layer h-BN dielectric films on metal substrates.[18] In previous work, the goal has been to achieve BN films with uniform thickness across the entire sample. Here, we use growth conditions that cause a partial wetting of the BN film on the Ru substrate to generate staircases of few-layer h-BN with extended (several μm) atomically flat terraces and thickness increasing in monolayer increments up to ~10 atomic layers. Characterized by AES excited by the focused electron beam of an ultrahigh-vacuum (UHV) SEM, these samples provide direct measurements of the thickness dependent intensity of Auger electrons from few-layer h-BN or the underlying substrate, which can be analyzed to extract the IMFP, $\lambda(E)$.

Hexagonal BN was grown on epitaxial Ru(0001) substrates by reactive magnetron sputtering of a solid B target in Ar/N_2 (ratio 4:1; total pressure: 10^{-2} Torr).[18] The epitaxial Ru(0001) thin film substrates were prepared *in situ*, following procedures described previously.[19] The h-BN films were investigated using an UHV-SEM (Zeiss Gemini UHV) and nano-Auger electron spectroscopy (Omicron Nanoprobe)[20] at 3 keV incident electron beam energy and a beam current between 300 pA and 3 nA. The surface microscopy and spectroscopy was complemented by high-resolution transmission electron microscopy (TEM) in an aberration-corrected microscope (FEI Titan 80–300) of cross-sections prepared by focused ion-beam milling combined with lift-off techniques.[21]

The negligible chemical reactivity and low sticking coefficient of h-BN poses substantial challenges in realizing the controlled synthesis of h-BN films beyond monolayer thickness. Uniform few-layer h-BN films have been formed by reactive magnetron sputtering via alternating low-temperature deposition and crystallization at high temperatures.[18] Deposition of several atomic layers by magnetron sputtering followed by annealing at high temperature ($>900\,^{\circ}$C) produces partially dewetted crystalline h-BN. Figure 1(a) shows an overview of the typical morphology of these films. The substrate is covered by large (up to ~100 μm base size) aggregates of few-layer h-BN. A zoomed-in view demonstrates that these islands consist of a well-defined stack of individual sheets (Fig. 1(b)). Additional characterization shows that the thickness of these layer stacks varies from 1 atomic layer near the periphery to ~10 atomic layers in monolayer increments. Sections with uniform thickness often comprise large, atomically flat terraces. Auger electron spectroscopy, discussed below, shows that the areas between the h-BN islands consist of bare Ru metal, not covered by h-BN.

Cross-sectional TEM results are consistent with the conclusions drawn from surface imaging by SEM. Overview TEM images show the overall sample structure consisting of the sapphire substrate, epitaxial Ru(0001) film and few-layer h-BN near the surface (Fig. 2(a)). High-resolution cross-sectional TEM demonstrates a high degree of crystallinity of the layered BN film (Fig. 2(b)), whose thickness reaches up to ~20 atomic layers in some areas. Comparing experimental high-resolution images with multislice TEM image simulations, we find that the BN film is predominantly A-A′-A stacked, i.e., shows the stacking sequence of hexagonal BN. After several atomic layers with perfect h-BN stacking, the sequence is interrupted by stacking faults (Fig. 2(c)), but the layered structure persists throughout the film. In most cases, the in-plane orientation of the layers is preserved across stacking faults, but occasionally we find that the characteristic high-resolution contrast becomes blurred, suggesting an in-plane rotation in these layers.

UHV SEM of stepped few-layer h-BN stacks (Fig. 3(a)) shows that secondary electron intensity maps provide a convenient tool to track local changes in h-BN thickness. Analyzing the image contrast, we find that the secondary electron intensity is proportional to the number of BN layers (Fig. 2(b)) over a wide thickness range, extending to at least 10 atomic layers (the thickest film

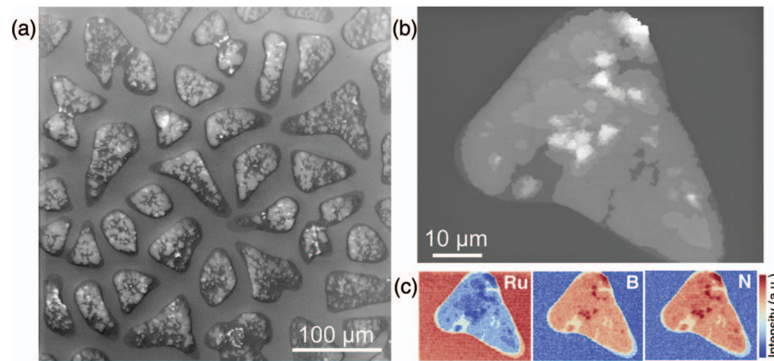

FIG. 1. Partially wetting h-BN islands with large atomically flat terraces on Ru. (a) UHV SEM image of an array of BN islands on epitaxial Ru(0001)/Al_2O_3(0001). (b) High-magnification view of one of the h-BN islands showing large, atomically flat terraces in which the BN thickness is constant. For this particular island, the thickness varies in single-layer steps from 1 to 6 atomic layers. (c) Chemical maps, obtained by UHV nano-Auger electron spectroscopy (AES) of Ru_{MNN}, B_{KLL}, and N_{KLL} Auger lines, respectively. False color scale: blue—low; red—high intensity. Note the increased B and N AES signal coinciding with higher secondary electron intensity in areas with thicker h-BN, and the contrast inversion between the B/N and Ru AES maps.

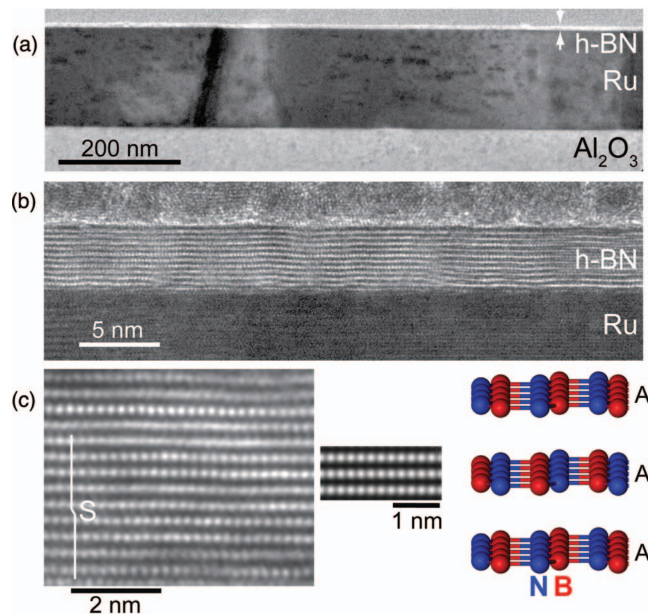

FIG. 2. TEM imaging of few-layer h-BN stacks on Ru(0001). (a) Overview image. (b) 12-layer h-BN section. (c) Left: High-magnification view, showing predominantly h-BN (A-A′-A) stacking with occasional stacking faults (S). Center: TEM image simulation for h-BN with A-A′-A stacking. Right: Ball-and-stick model of A-A′-A stacked h-BN.

sections probed here). Only very thin films (i.e., monolayer h-BN) deviate from this behavior. We find that the transition from bare Ru(0001) to single-layer h-BN is accompanied by a small increase in the secondary electron intensity, whereas each subsequent h-BN layer causes a much larger (and constant) increment. This reflects the fact that the interaction with the substrate and the moiré structure give monolayer h-BN/Ru(0001) distinct electronic and chemical properties,[15] whereas with the completion of the second layer bulk-like h-BN properties are reached.[18] The observed linear intensity increase implies that the SEM contrast is sensitive to monolayer changes in film thickness. From the fact that thicker areas give rise to higher secondary electron intensity, we conclude that the detected secondary electrons originate primarily in the h-BN layer, and the linear increase suggests that the total intensity is the sum of contributions from the individual atomic layers of the film, consistent with a large escape depth of the energetic secondary electrons. This behavior

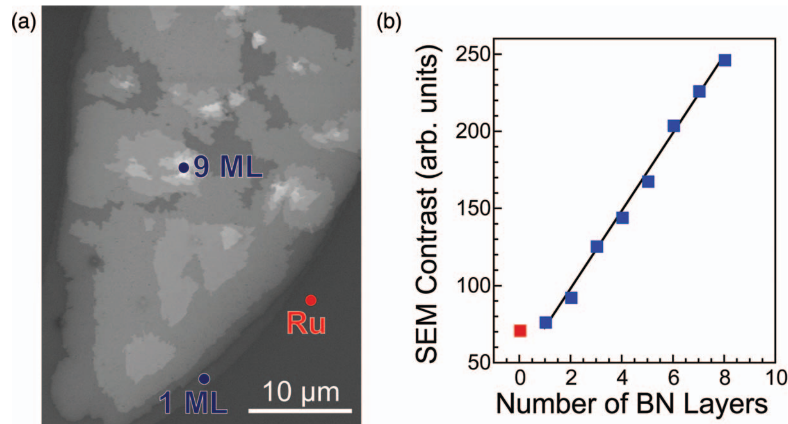

FIG. 3. Quantification of the thickness-dependent SEM contrast of few-layer h-BN on Ru(0001). (a) UHV SEM image (3 keV, 300 pA) of a h-BN island with stepwise thickness increase from 1 to 9 atomic layers. (b) Analysis of the secondary electron intensity as a function of h-BN thickness, measured in (a).

is different from that observed for few-layer graphene on Ru, where the secondary electron intensity decreases for thicker graphene films, implying that the detected secondary electrons originate in the Ru substrate and are attenuated by the graphene sheets.[22] A possible origin of the difference between graphene and h-BN is the partially ionic character of h-BN, in contrast to the purely covalent bonding of C atoms in graphene.

In addition to monitoring monolayer thickness variations, which are conveniently mapped by SEM, the characterization of few-layer h-BN requires absolute thickness measurements. Previous reports for graphene have shown that Auger electron spectroscopy (AES) can be used to routinely determine film thickness.[23] However, precise values of the inelastic mean free path Auger electrons are required for a quantitative thickness analysis. We have used our stepped BN stacks in conjunction with spatially resolved AES measurements on terraces with known film thickness to quantify the IMFP of Auger electrons in h-BN, and to identify a reliable method for measuring the thickness of h-BN films on metals. Figure 3 shows the results of such an AES measurement. As expected, the Auger lines of all three elements in our system, B_{KLL}, N_{KLL}, and Ru_{MNN}, show a systematic intensity change with increasing BN thickness: with the addition of each BN layer, the B_{KLL} and N_{KLL} signals increase in intensity, whereas thicker h-BN progressively attenuates the Ru_{MNN} intensity.

The spectra in Fig. 4 provide several independent measurements of the IMFP at different electron energy, which together yield λ(E) of h-BN. For Auger electrons originating in the h-BN film itself (B_{KLL} and N_{KLL} transitions), we assume that the electrons from the outermost h-BN layer reach the detector unattenuated (intensity I_0), whereas those from deeper layers undergo an exponentially depth dependent attenuation with IMFP λ. The intensity of the B_{KLL} and N_{KLL} Auger electrons from *n*-layer h-BN is then given by

$$I_n = I_0 \sum_{k=1}^{n} \exp\left[-\left(k-1\right)d / \lambda \sin\theta\right],$$

where d is the layer spacing in h-BN (3.3 Å) and $\theta = 45°$ is the takeoff angle in our AES system.

For Auger electrons originating in the Ru substrate (Ru_{MNN} transition), the analogous attenuation by *n*-layer h-BN from an initial intensity, $I_{Ru,0}$, to a final intensity at the surface, $I_{Ru,n}$ (after traversing *n* h-BN layers) is given by

$$I_{Ru,n} = I_{Ru,0} \exp\left[-nd / \lambda \sin\theta\right].$$

Figure 5(a) shows the result of this analysis of the measured B_{KLL}, Ru_{MNN}, and N_{KLL} Auger lines of few-layer h-BN on Ru(0001). The inelastic mean free path, λ(E), increases approximately linearly with the energy of the Auger electrons, similar to previous results for few-layer graphene.[23]

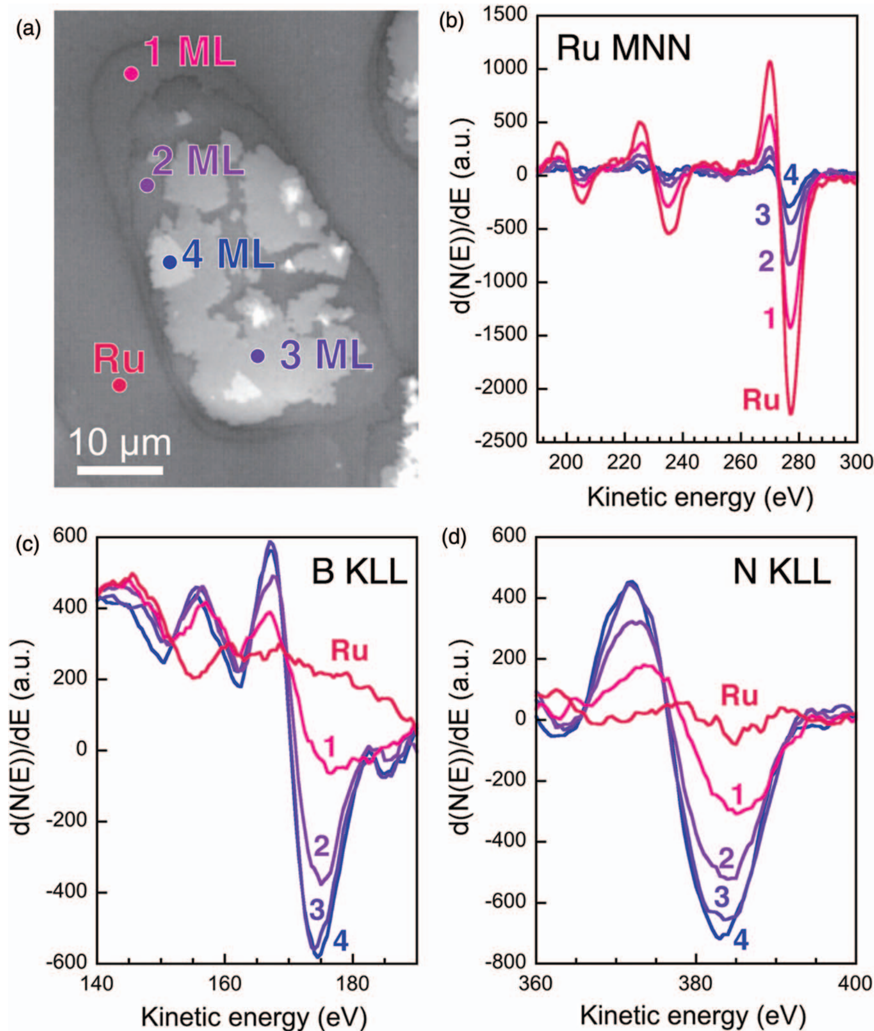

FIG. 4. Thickness dependence of the nano-Auger signal of few-layer h-BN on Ru(0001). (a) UHV SEM image (3 keV, 300 pA) of an island with stepwise thickness increase from 1 to 4 atomic layers h-BN. (b) Ruthenium MNN derivative AES signal; (c) Boron KLL AES signal; and (d) Nitrogen KLL AES signal as a function of h-BN thickness, measured at the points indicated in (a).

The IMFP varies slowly from $\lambda_{B\ KLL} = 7.5$ Å (∼2.3 layers BN) to $\lambda_{N\ KLL} = 9.5$ Å (close to 3 layers BN). Thus, measurements of the increase in the B_{KLL} or N_{KLL} AES intensity with thickness or the attenuation of the Ru_{MNN} Auger electrons provide similar conditions for h-BN thickness measurements. For h-BN transferred to SiO_2, the attenuation of the O_{KLL} AES intensity could additionally be used for thickness determination. From our results, we extrapolate an IMFP $\lambda_{O\ KLL} = 10.7$ Å (∼3.2 layers BN) at the energy of O_{KLL} Auger transition (∼500 eV). A comparison with the "universal curve" of energy-dependent electron escape depths (Fig. 5(b)) shows good general agreement, with the measured values of the IMFP in h-BN lying somewhat above the "universal curve" but well within the scatter of individual IMFP values.[24] Finally, our measurements allow us to estimate the range of h-BN thicknesses that can be measured by AES. Tracking the intensity of the N_{KLL} transition, and assuming that intensity changes of 5% can be detected in the derivative spectra, AES measurements can provide reliable thickness measurements for h-BN films of 1 to 6 atomic layers.

In conclusion, we have used large, partially wetting islands of stacked h-BN layers on Ru(0001) to explore electron-based approaches for determining the thickness of few-layer h-BN films. We find that the intensity of secondary electrons in scanning electron microscopy depends linearly on

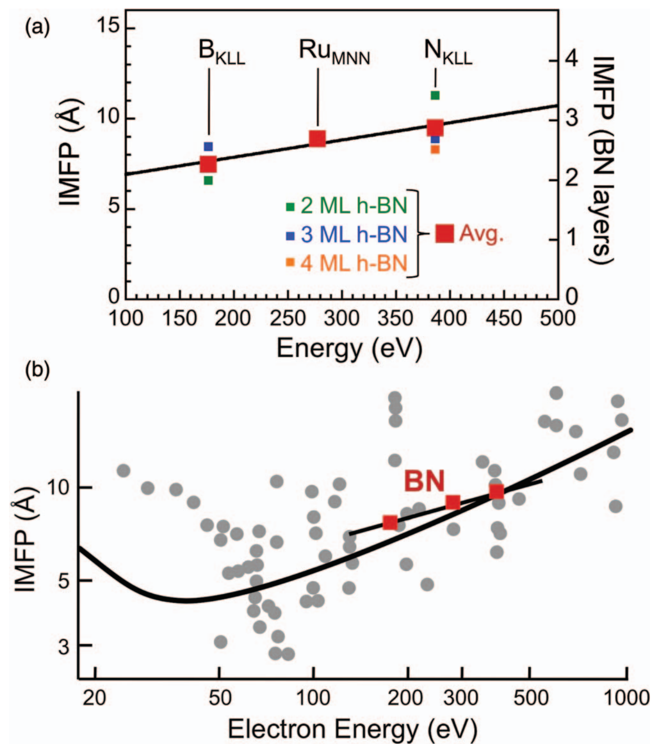

FIG. 5. Analysis of the energy dependent inelastic mean-free path λ(E) of Auger electrons in few-layer h-BN. (a) IMFP derived from an analysis of B_{KLL}, Ru_{MNN}, and N_{KLL} Auger intensities as a function of BN thickness. Small symbols denote values derived for 2, 3, and 4 layer BN on Ru(0001). Large symbols represent the average of these values. Line: linear fit to the averages. (b) IMFP for BN plotted with the "universal curve." Adapted from Ref. 24.

the number of h-BN layers up to thicknesses of at least 10 layers. SEM thus provides a simple and sensitive means of tracking thickness variations in h-BN films, giving robust contrast for monolayer changes in thickness. Within a limited thickness range from 1 to ∼6 BN atomic layers, Auger electron spectroscopy provides an absolute film thickness measurement if referenced against a proper standard, for example, monolayer or bulk h-BN. Evidently, the reference standard should be as close as possible to the structure and composition of the sample whose thickness is to be determined. In practice, a h-BN monolayer grown by CVD on a metal substrate should represent a convenient reference, since attributes such as perfect stoichiometry, full substrate coverage, and uniform thickness and density are relatively easy to achieve. With such a standard, possible sources of uncertainty, for instance in routine thickness measurements while developing synthesis approaches for few-layer h-BN, would be variations in the composition, crystal quality, or adsorbates on the surface of the few-layer samples. The primary utility of AES thickness metrology lies in the fact that the measurement is quite generally applicable, independent of the material of the substrate supporting the h-BN film. AES thus provides a versatile complement to other methods, e.g., optical reflectivity, which require a special substrate.

Research carried out at the Center for Functional Nanomaterials, Brookhaven National Laboratory, which is supported by the U.S. Department of Energy, Office of Basic Energy Sciences, under Contract No. DE-AC02–98CH10886.

[1] K. S. Novoselov, D. Jiang, F. Schedin, T. J. Booth, V. V. Khotkevich, S. V. Morozov, and A. K. Geim, Proc. Natl. Acad. Sci. U.S.A. **102**(30), 10451–10453 (2005).
[2] F. Xia, D. B. Farmer, Y.-M. Lin, and P. Avouris, Nano Lett. **10**(2), 715–718 (2010).
[3] A. Splendiani, L. Sun, Y. Zhang, T. Li, J. Kim, C.-Y. Chim, G. Galli, and F. Wang, Nano Lett. **10**(4), 1271–1275 (2010).
[4] W. Jin, P.-C. Yeh, N. Zaki, D. Zhang, J. T. Sadowski, A. Al-Mahboob, A. M. van der Zande, D. A. Chenet, J. I. Dadap, I. P. Herman, P. Sutter, J. Hone, and R. M. Osgood, Phys. Rev. Lett. **111**(10), 106801 (2013).
[5] K. Watanabe, T. Taniguchi, T. Niiyama, K. Miya, and M. Taniguchi, Nat. Photonics **3**(10), 591–594 (2009).

[6] J. Xue, J. Sanchez-Yamagishi, D. Bulmash, P. Jacquod, A. Deshpande, K. Watanabe, T. Taniguchi, P. Jarillo-Herrero, and B. J. LeRoy, Nat. Mater. **10**, 282–285 (2011).
[7] C. R. Dean, A. F. Young, I. Meric, C. Lee, L. Wang, S. Sorgenfrei, K. Watanabe, T. Taniguchi, P. Kim, K. L. Shepard, and J. Hone, Nat. Nanotechnol. **5**(10), 722–726 (2010).
[8] L. Wang, I. Meric, P. Y. Huang, Q. Gao, Y. Gao, H. Tran, T. Taniguchi, K. Watanabe, L. M. Campos, D. A. Muller, J. Guo, P. Kim, J. Hone, K. L. Shepard, and C. R. Dean, Science **342**(6158), 614–617 (2013).
[9] G.-H. Lee, Y.-J. Yu, X. Cui, N. Petrone, C.-H. Lee, M. S. Choi, D.-Y. Lee, C. Lee, W. J. Yoo, K. Watanabe, T. Taniguchi, C. Nuckolls, P. Kim, and J. Hone, ACS Nano **7**(9), 7931–7936 (2013).
[10] L. Britnell, R. V. Gorbachev, R. Jalil, B. D. Belle, F. Schedin, A. Mishchenko, T. Georgiou, M. I. Katsnelson, L. Eaves, S. V. Morozov, N. M. R. Peres, J. Leist, A. K. Geim, K. S. Novoselov, and L. A. Ponomarenko, Science **335**(6071), 947–950 (2012).
[11] R. V. Gorbachev, I. Riaz, R. R. Nair, R. Jalil, L. Britnell, B. D. Belle, E. W. Hill, K. S. Novoselov, K. Watanabe, T. Taniguchi, A. K. Geim, and P. Blake, Small **7**(4), 465–468 (2011).
[12] D. Golla, K. Chattrakun, K. Watanabe, T. Taniguchi, B. J. LeRoy, and A. Sandhu, Appl. Phys. Lett. **102**, 161906 (2013).
[13] A. Nagashima, N. Tejima, Y. Gamou, T. Kawai, and C. Oshima, Phys. Rev. Lett. **75**(21), 3918–3921 (1995).
[14] M. Corso, W. Auwarter, M. Muntwiler, A. Tamai, T. Greber, and J. Osterwalder, Science **303**(5655), 217–220 (2004).
[15] P. Sutter, J. Lahiri, P. Albrecht, and E. Sutter, ACS Nano **5**(9), 7303–7309 (2011).
[16] L. Song, L. Ci, H. Lu, P. B. Sorokin, C. Jin, J. Ni, A. G. Kvashnin, D. G. Kvashnin, J. Lou, B. I. Yakobson, and P. M. Ajayan, Nano Lett. **10**(8), 3209–3215 (2010).
[17] Y. Shi, C. Hamsen, X. Jia, K. K. Kim, A. Reina, M. Hofmann, A. L. Hsu, K. Zhang, H. Li, Z.-Y. Juang, M. S. Dresselhaus, L.-J. Li, and J. Kong, Nano Lett. **10**(10), 4134–4139 (2010).
[18] P. Sutter, J. Lahiri, P. Zahl, B. Wang, and E. Sutter, Nano Lett. **13**(1), 276–281 (2013).
[19] P. W. Sutter, P. M. Albrecht, and E. A. Sutter, Appl. Phys. Lett. **97**(21), 213101 (2010).
[20] P. Sutter, R. Cortes, J. Lahiri, and E. Sutter, Nano Lett. **12**(9), 4869–4874 (2012).
[21] E. Sutter, P. Albrecht, B. Wang, M. L. Bocquet, L. J. Wu, Y. M. Zhu, and P. Sutter, Surf. Sci. **605**(17–18), 1676–1684 (2011).
[22] P. W. Sutter, J.-I. Flege, and E. A. Sutter, Nat. Mater. **7**(5), 406–411 (2008).
[23] Mingsheng Xu, D. Fujita, J. Gao, and N. Hanagata, ACS Nano **4**, 2937–2945 (2010).
[24] M. P. Seah and W. A. Dench, Surf. Interface Anal. **1**, 2–11 (1979).